

Anomalous Impact of Surface Wettability on Leidenfrost Effect at Nanoscale

Yue Wang(王玥)^{1,2}, Xiaoxiang Yu(余晓翔)^{1,2}, Xiao Wan(万骁)^{1,2},
Nuo Yang(杨诺)^{1,2}, and Chengcheng Deng(邓程程)^{1,2*}

¹*School of Energy and Power Engineering, Huazhong University of Science and Technology, Wuhan 430074, China*

²*State Key Laboratory of Coal Combustion, Huazhong University of Science and Technology, Wuhan 430074, China*

(Received 1 June 2021; accepted 5 August 2021; published online 2 September 2021)

Leidenfrost effect is a common and important phenomenon which has many applications, however there is a limited body of knowledge about the Leidenfrost effect at the nanoscale regime. We investigate the impact of substrate wettability on Leidenfrost point temperature (LPT) of nanoscale water film via molecular dynamics simulations, and reveal a new mechanism different from that at the macroscale. In the molecular dynamics simulations, a method of monitoring density change at different heating rates is proposed to obtain accurate LPT under different surface wettability. The results show that LPT decreases firstly and then increases with the surface wettability at the nanoscale, which is different from the monotonous increasing trend at the macroscale. The mechanism is elucidated by analyzing the competitive effect of adhesion force and interfacial thermal resistance, as well as different contributions of gravity on LPT at the nanoscale and macroscale. The investigations can deepen the understanding of Leidenfrost effect at the nanoscale regime and also facilitate to guide the applications of heat transfer and flow transport.

DOI: 10.1088/0256-307X/38/9/094401

Leidenfrost effect is a classical fluid phenomenon which occurs when a liquid is deposited on a highly superheated surface and a layer of vapor is formed immediately between the liquid and the substrate surface.^[1] Due to the formation of the vapor layer, the liquid suspends above the substrate and the direct heat transfer is isolated or reduced. The transition temperature at which Leidenfrost effect occurs is called Leidenfrost point temperature (LPT). During the early stage, the research about Leidenfrost effect mainly focused on experimental measurements^[2–5] and theoretical research.^[6,7] Afterwards, Leidenfrost effect has been widely studied for many applications on the macro scale, such as cooling,^[8–10] liquid transport,^[11–14] and drag reduction.^[15,16]

Due to the plentiful applications, there are many studies of the Leidenfrost effect that focus on adjusting the LPT for different uses. In recent heat transfer studies, through depositing nanoparticles or other nanostructures on a macro-scale surface, the LPT can be significantly increased, which can be used to accelerate the cooling of overheating objects.^[17–20] Some studies also indicated that the LPT can be decreased by a micropatterned surface.^[21,22] In addition, electrostatic liquid attraction has also been applied to suppress Leidenfrost effect and prevent surface from drying out, even at 500 °C.^[23] Furthermore, some studies have been carried out to decrease the LPT for saving energy in applications that take advantage of the Leidenfrost effect for drop control or drag reduc-

tion. Moreover, there are some studies on the impact of surface wettability on Leidenfrost effect at the macroscale, which concludes that the LPT on hydrophobic surfaces is much lower than that on hydrophilic surface.^[24–26]

In spite of abundant investigations of the Leidenfrost effect at the macroscale, there is a limited knowledge about the mechanism of Leidenfrost effect at the nanoscale. The experimental study of the Leidenfrost effect at the nanoscale is hard to be carried out due to the difficulty of measurement technology. In recent years, attempts have been made to study the levitation mechanism and liquid-solid intermolecular force^[27] and the kinetic properties^[28] in nanoscale Leidenfrost effect by molecular models. Some researchers found that LPT at the nanoscale presented inconsistent law with that at the macroscale through simulations. For example, due to a strong liquid-solid intermolecular force, the LPT at the nanoscale was found to be significantly decreased, because an adsorption layer was formed by strong intermolecular force, which exceeded the critical temperature of the liquid molecule and promoted heat transfer between the heated wall and nanodroplet.^[29] This finding is also confirmed in the simulation of nanoscale Leidenfrost effect, which has found the occurrence of Leidenfrost point only at 373 K, much lower than the LPT observed at 473 K for macroscale measurement.^[30] Since the Leidenfrost effect plays an important role in many applications and its mechanism at the nanoscale is am-

Supported by the National Key Research and Development Program of China (Grant No. 2018YFE0127800).

*Corresponding author. Email: dengcc@hust.edu.cn

© 2021 Chinese Physical Society and IOP Publishing Ltd

biguous, it is necessary to study the Leidenfrost effect at the nanoscale and to explore the essential mechanism at the atomic level.

In this work, impact of surface wettability on Leidenfrost effect at nanoscale is studied by molecular dynamics simulation. Firstly, the simulation system of water film heated on substrates with different wettability is established, and the molecular dynamics simulation method is described. Secondly, a simulation method of monitoring density change is proposed to obtain accurate LPT under different surface wettability. Thirdly, the results are analyzed and discussed, and the mechanism is explained by comparing the interfacial thermal resistance and adhesion force, as well as the gravity impact.

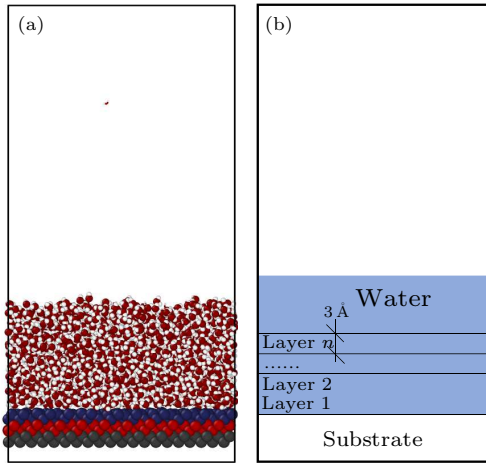


Fig. 1. (a) The simulation system. (b) Schema of the division of water layers used to compute the mass density of water film above the substrate. The average mass density of molecules within the layer is calculated as a function of the distance away from the substrate.

Table 1. Molecular interaction parameters used in this molecular dynamics (MD) simulation.

Molecular pair	σ (Å)	ε (eV)	q (e)
O–O	3.16435	0.0068355	–1.0484
H–H	0	0	0.5242
Substrate–Substrate	2.905	2.168201	0

Simulation System and Method. We use the equilibrium molecular dynamics (EMD) simulation method,^[31,32] which has been widely used to calculate nanoscale thermal transport properties.^[33–35] The EMD simulations in this work are performed by the large-scale atomic/molecular massively parallel simulator (LAMMPS) package.^[36,37] The Stillinger–Weber (SW) force field is used for substrate molecules, TIP4P force field^[38–40] is used for water molecules, and the Lennard–Jones (LJ) potential is used for interaction between substrate and water molecules. As same as previous simulation,^[41] the potential well depth of LJ potential is modified artificially to change the wettability of substrate. The molecular interaction parameters used in this MD simulation are listed

in Table 1, which is set up with reference to previous study.^[41] Periodic boundary conditions are applied in all three dimensions. The velocity Verlet algorithm is employed to integrate equations of motion.^[42] Here, 1 fs and 10 Å are chosen as time step and cutoff distance, respectively, for the Lennard–Jones interaction. In addition, six independent simulations with different initial conditions are conducted to get statistical average results. The configurations of simulation system are visualized by visual molecular dynamics (VMD), as shown in Fig. 1.

The simulation system is composed of two parts, namely nanoscale water film and substrate. In all cases, the thickness of the water film is 2.5 nm, and the substrate is divided into six layers and different layers match with different functions. As shown in Fig. 1(a), the bottom two layers of substrate atoms stayed still as a boundary wall to keep the system volume constant which is called fixed layer. The middle two layers were set as heat source via a Langevin thermostat from which heat flux was generated, called the heating layer. The top two layers were set to be surface considered as the real atoms, which is called the real layer, through which the heat is transferred to the liquid water. The dimensions of simulation domain are $54.3 \times 54.3 \times 100 \text{ \AA}^3$, and a virtual reflecting wall, which will bound the molecules back specularly when they collide the wall, is placed at the top to seal the simulation box in the Z axis. No energy transfer will occur through the interaction between molecules and this wall. The water density is kept at 1.0 g/cm^3 . The TIP4P water model is used with the SHAKE^[43] algorithm to constrain the bond lengths and angles. The following equation is used to describe the interaction of water molecular:

$$U_{ab} = \sum_i^a \sum_j^b \frac{k_C q_{a_i} q_{b_j}}{r_{a_i b_j}} + \sum_i^a \sum_j^b 4\varepsilon_{a_i b_j} \left[\left(\frac{\sigma_{a_i b_j}}{r_{a_i b_j}} \right)^{12} - \left(\frac{\sigma_{a_i b_j}}{r_{a_i b_j}} \right)^6 \right], \quad (1)$$

where the first term on the right side is Coulomb force, and the second term is the LJ potential;^[44] a and b denote different H_2O molecules, subscript i and j represent different atom types (hydrogen or oxygen) in each H_2O molecule. The form of summation represents the computation over all the interaction forces of each type of atoms (denoted by i or j) within each H_2O molecule (denoted by a or b). A particle-particle mesh solver is used, which can handle long-range Coulombic interactions for periodic systems with slab geometry.

In this simulation, the system is firstly equilibrated with given thermostat until the temperature of water system reaches a stable value of 293 K, then the sub-

strate is heated to specified temperatures to determine the Leidenfrost point. Afterwards, the liquid water at initial 293 K is heated on the hot substrate. The entire system is integrated with NVE ensemble during the simulation and the substrate is still controlled at the desired temperature.

In order to obtain the detailed results, the whole simulation box is divided into several slices parallel to the substrate surface, and the average density and temperature of the molecules in each layer is respectively calculated. Figure 1(b) illustrates the scheme used to compute the density and temperature inside different layers above the substrate. Each layer is set to thickness of 3 Å, which is divided according to the thickness of water film to properly present the density change.

Interfacial thermal resistance and adhesion force between water film and substrate are calculated to analyze the results by using nonequilibrium MD simulations.^[45] Adhesion force refers to the ability of water film adhered to the substrate surface, which is determined by a computation of the interaction force between water molecules and the substrate. During the process of water film wetting the substrate, adhesion force is calculated by integrating the interaction forces over time and average the results when it reaches a stable period. Then, the initial conditions are changed to repeat the calculations to obtain a statistical average result. The heat flux (q) is calculated by averaging the energy input and output rates from the heat source and sink. The temperature jump (ΔT) across the interface is defined by the temperature difference between the water film and substrate. The interfacial thermal resistance (R_κ) is then calculated by $R_\kappa = \Delta T/q$.

In the TIP4P model, water molecules interact with substrate surface only by van der Waals interactions between substrate and oxygen. The interatomic potential between substrate and oxygen atoms is given by the well-known LJ potential as follows:

$$U = 4\varepsilon \left[\left(\frac{\sigma}{r} \right)^{12} - \left(\frac{\sigma}{r} \right)^6 \right]. \quad (2)$$

According to the previous related simulation,^[46] the interaction parameters between the substrate (silicon atoms) and oxygen atoms of water are given in Table 2. Here, the potential well depth ε of the LJ potential is modified artificially to change the wettability of substrate for five different cases. In order to intuitively quantify the wettability of substrate with different values of potential well depth, the contact angles (θ_c) of water molecules wetting the substrate at room temperature are respectively calculated for five different cases. As shown in Fig. 2, different wettability of substrates is presented changing from hydrophobic to hydrophilic.

Table 2. Interaction parameters between substrate and oxygen atoms of water.

Molecular pair	ε (eV)	δ (Å)	Contact angle θ_c (deg)
Substrate-O	0.005	3.27	129.4
	0.0065	3.27	119.3
	0.008	3.27	97.3
	0.009	3.27	81.5
	0.01	3.27	62.9

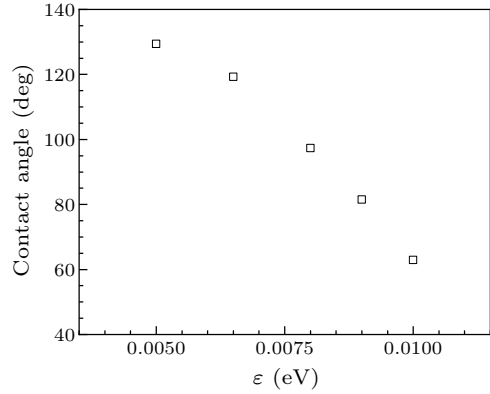


Fig. 2. Contact angle versus ε , with different wettability characterized by the exhibited contact angle between water and substrate.

Results and Discussions. We propose a simulation method of monitoring density change at different heating rates to obtain accurate LPT under different surface wettability. The density of water film is firstly calculated in the first three layers hithermost to the substrate. By monitoring density change we can define the exact time of the occurrence of the levitation of water film. Owing to the balance between the cutoff radius and height of the layers of the control volumes, the density of water film in first three layers within the cutoff radius obviously decreases, which means the occurrence of the water film levitation in this MD study. According to this judgment sign, the moment of the occurrence of the Leidenfrost effect can be determined by the time when the water film begins to levitate.

Figure 3 shows the procedure of monitoring water film's density change to obtain LPT for two substrates with different wettability. Since the surface wettability is usually characterized by contact angle, here we choose a contact angle of 129.4° to represent the hydrophobic substrate, and a contact angle of 62.9° to represent the hydrophilic substrate. Firstly, the substrate is in a slow heating process, from low temperature (below LPT) to high temperature (above LPT), and the corresponding LPT can be determined by monitoring water film's density change. Figure 3(a) shows the density change of water film on the hydrophobic substrate (129.4°). When water film at the room temperature comes into contacting with hot substrate, the density of water film in the first layer is very low due to the hydrophobicity, and the density of water film in the second layer and the third layer is normal as the liquid water density. During initial con-

tact with the hot substrate, the water film has a rapid evaporation which results in a sudden drop in density. Subsequently, due to the weak adhesion force between substrate and water, water film appears bouncing up and down, until the substrate temperature rises to the LPT, at which the vapor layer appears and the density of the water layer drops sharply. Once the Leidenfrost effect occurs, the water film does not stay near the substrate and continues to rise. For the case of hydrophilic substrate (62.9°), as shown in Fig. 3(b), there is also a sharp drop in the density curve, which is almost consistent with the phenomena shown in Fig. 3(a). Because of different adhesion forces between substrate and water, there is some minor difference for the two cases with different surface wettability.

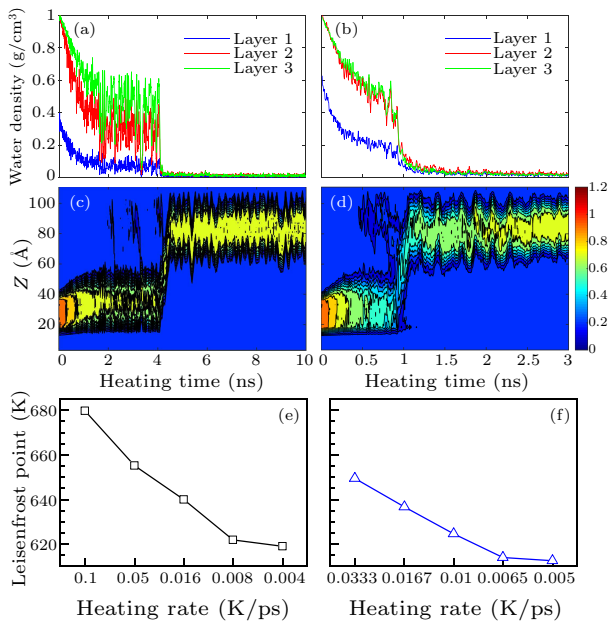


Fig. 3. Procedure of monitoring water film's density change to obtain LPT for two substrates with different wettability. The first three-layer water density change with heating time: (a) for the hydrophobic substrate (contact angle 129.4°), (b) for the hydrophilic substrate (contact angle 62.9°); cloud maps of water film density: (c) for the hydrophobic substrate (contact angle 129.4°), (d) for the hydrophilic substrate (contact angle 62.9°); LPT converge with heating rate: (e) for the hydrophobic substrate (contact angle 129.4°), (f) for the hydrophilic substrate (contact angle 62.9°).

The corresponding cloud maps of water film density for the two cases are shown in Figs. 3(c) and 3(d), which reflect the movement trajectory of the water film in the Z direction with the heating time of the substrate, where the color represents the density value of water film. It can be found that the results of cloud maps of density are consistent with the results of density change of water film as shown in Figs. 3(a) and 3(b). Before the occurrence of Leidenfrost effect, the nucleation boiling will first occur when the water film is heated by the hot substrate, and bubbles will be generated in the nucleation boiling. The appearance

of bubbles will lead to a temporary density decrease of water layer, and when the bubbles escape, the density of water layer will rise again. Therefore, drastic fluctuations in water density can be observed as shown in Fig. 3.

Since the substrate is in a process of heating up and the heat transfer process takes time, the LPT obtained by this method has a certain lag. By slowing down the heating rate of the substrate, as shown in Figs. 3(e) and 3(f), it can be found that the LPT tends to converge, thus an accurate LPT can be obtained by the converge value.

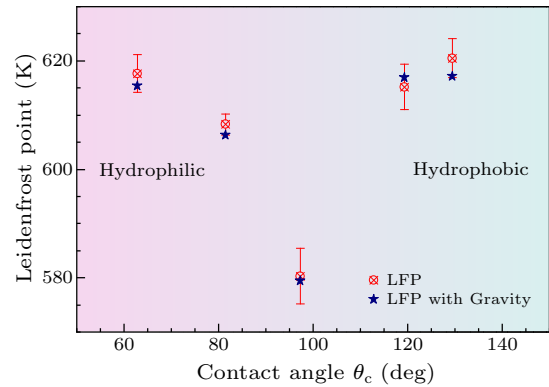


Fig. 4. LPT with different surface wettability (characterized by contact angles) at the nanoscale.

With the above-mentioned methods, we obtained the LPTs of five substrates with different surface wettability characterized by different contact angles, as shown in Fig. 4. It can be found that the LPT decreases firstly and then increases with the contact angle in MD study at nanoscale, which is different from the monotonous increasing trend at the macroscale.^[47] In previous studies, it has been found that the LPT of water droplets at the nanoscale is much lower than that at the macroscale.^[30] Therefore, for the Leidenfrost effect, there are indeed some differences between nanoscale and macroscale phenomena. Thus, it is worth exploring in-depth mechanism of causing the difference between nanoscale and macroscale. The result shows that the gravity of nanoscale water film is far smaller than the adhesion force between water film and substrate. To determine the effect of gravity at the nanoscale, the results without gravity (represented by the red circles in Fig. 4) are compared with those with gravity (represented by the blue stars in Fig. 4). It is concluded that the effect of gravity is completely negligible, and the gravity indeed has almost no impact on the results of LPT at the nanoscale as in Fig. 4.

In order to explain the mechanism of the impact of surface wettability on Leidenfrost effect at the nanoscale, the adhesion force and the interfacial thermal resistance, as well as the gravity, are calculated and compared. As shown in Fig. 5, the adhesion force

is represented by black square, the interfacial thermal resistance is represented by blue triangle which is in good agreement with the previous study represented by green star,^[45] and the gravity of water is represented by red circle. On the one hand, due to the existence of adhesion force, the water film needs to overcome the adhesion force to suspend above the substrate and to reach the Leidenfrost state, therefore LPT increases with the increase of adhesion force. On the other hand, interface thermal resistance hinders the heat conduction between substrate and water. Because the sufficient heat is required to produce the vapor layer, LPT increases as the interfacial thermal resistance increases. As the substrate becomes more hydrophobic (contact angle becomes larger), the adhesion force between the substrate and the water decreases which will result in a lower LPT, while the interface thermal resistance increases which will result in a higher LPT. Therefore, the impact of surface wettability on Leidenfrost effect is the competitive effect of adhesion force and interfacial thermal resistance, which results in the non-monotonic trend as shown in Fig. 4.

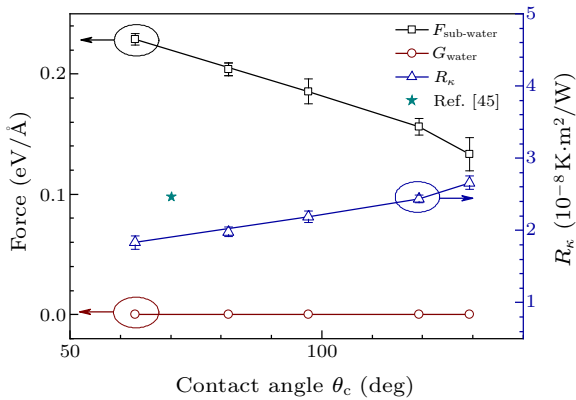


Fig. 5. The effect of adhesion force and interfacial thermal resistance, as well as gravity, for different surface wettability (contact angles).

In addition to the synergistic effect of adhesion force and interfacial thermal resistance, the impact of gravity contributes to the difference between nanoscale and macroscale. As shown in Fig. 6, the ratios of adhesion force and gravity are given for macroscale and nanoscale. Generally speaking, the nanoscale usually refers to the size of 1–100 nm; the macroscale is usually more than tens of micrometers. By comparing the ratio of adhesion force and gravity at macroscale and nanoscale, it can be seen that the gravity of water at the nanoscale is negligible due to the relatively large specific surface, so the gravity has almost no impact on the LPT at the nanoscale which has been confirmed by the previous results in Fig. 4. However, for the macroscale, the gravity and adhesion force are comparable, like the macroscale result in Fig. 6, which is obtained based on the experimen-

tal data in the previous macroscale study.^[48] Thus, the contribution of water’s gravity to the Leidenfrost effect at the macroscale cannot be ignored. For the macroscale, the additive effect of gravity and adhesion force is far larger than the effect of interfacial thermal resistance on LPF. Therefore, the more hydrophobic the surface is, the smaller the adhesion force is, which can form steady suspended vapor film more easily, then the Leidenfrost effect is more likely to occur, which means that LPF changes monotonously with surface wettability at macroscale. However, for the nanoscale, since the effect of gravity can be ignored, the effects of adhesion force and interfacial thermal resistance are comparable. Therefore, the competition between the two effects leads to the non-monotonic change of LPF with surface wettability at nanoscale.

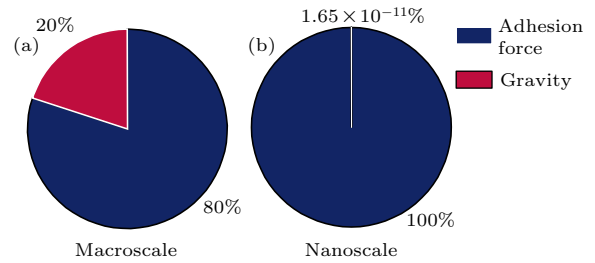


Fig. 6. The ratio of adhesion force and gravity for different scales: (a) macroscale, (b) nanoscale.

In summary, the impact of surface wettability on Leidenfrost effect at nanoscale is studied via molecular dynamics simulation. The mechanism of a new phenomenon found at nanoscale is elucidated. We propose a method of monitoring density change at different heating rates to obtain accurate LPTs under different surface wettability through MD simulations. A sharp decrease of the density is observed in the vicinity of the substrate, which can well predict the occurrence of Leidenfrost effect. The results show that LPT decreases firstly and then increases with the surface wettability defined by contact angles at nanoscale, which is different from the monotonous increasing trend at the macroscale. The mechanism is explored by analyzing the adhesion force and the interfacial thermal resistance between water film and substrate, as well as the impact of gravity. The gravity of water at nanoscale is negligible due to the relatively large specific surface, while the gravity cannot be ignored at the macroscale. Thus, for the macroscale, the additive effect of gravity and adhesion force is far larger than the effect of interfacial thermal resistance on LPF, which results in a monotonous LPF change with surface wettability at macroscale. However, for the nanoscale, the effects of adhesion force and interfacial thermal resistance are comparable, and the competition between these two effects leads to a non-monotonic change of LPF with wettability at the nanoscale. This work reveals a new phenomenon of

Leidenfrost effect at the nanoscale, which will be helpful for many related applications such as designing anti-dragging surfaces, self-propelling droplets, self-assembled nano structures, and thermal management.

Acknowledgment. The authors thank the National Supercomputing Center in Tianjin (NSCC-TJ) and China Scientific Computing Grid (ScGrid) for providing assistance in computations.

References

- [1] Leidenfrost J G 1966 *Int. J. Heat Mass Transfer* **9** 1153
- [2] Bianco A L, Clanet C and Quéré D 2003 *Phys. Fluids* **15** 1632
- [3] Gottfried B, Lee C and Bell K 1966 *Int. J. Heat Mass Transfer* **9** 1167
- [4] Temple-Pediani R W 1969 *Proc. Inst. Mech. Eng.* **184** 677
- [5] Bernardin J D and Mudawar I 1999 *J. Heat Transfer* **121** 894
- [6] Gottfried B S and Bell K J 1966 *Ind. Eng. Chem. Fundamen.* **5** 561
- [7] Zhang S and Gogos G 1991 *J. Fluid Mech.* **222** 543
- [8] Quéré D 2013 *Annu. Rev. Fluid Mech.* **45** 197
- [9] Van Limbeek M A J, Schaarsberg M H K, Sobac B, Rednikov A, Sun C, Colinet P and Lohse D 2017 *J. Fluid Mech.* **827** 614
- [10] Raudensky M and Horsky J 2005 *Ironmak. Steelmak.* **32** 159
- [11] Jia Z H, Chen M Y and Zhu H T 2017 *Appl. Phys. Lett.* **110** 091603
- [12] Lagubeau G, Le M M, Clanet C and Quéré D 2011 *Nat. Phys.* **7** 395
- [13] Linke H, Alemán B J, Melling L D, Taormina M J, Francis M J, Dow-Hygelund C C, Narayanan V, Taylor R P and Stout A 2006 *Phys. Rev. Lett.* **96** 154502
- [14] Li J, Hou Y, Liu Y, Hao C, Li M, Chaudhury M K, Yao S and Wang Z 2016 *Nat. Phys.* **12** 606
- [15] Vakarelski I U, Berry J D, Chan D Y and Thoroddsen S T 2016 *Phys. Rev. Lett.* **117** 114503
- [16] Vakarelski I U, Chan D Y and Thoroddsen S T 2014 *Soft Matter.* **10** 5662
- [17] Sajadi S M, Irajizad P, Kashyap V, Farokhnia N and Ghasemi H 2017 *Appl. Phys. Lett.* **111** 021605
- [18] Kim H, DeWitt G, McKrell T, Buongiorno J and Hu L W 2009 *Int. J. Multiphas. Flow* **35** 427
- [19] Kim H, Truong B, Buongiorno J and Hu L W 2011 *Appl. Phys. Lett.* **98** 083121
- [20] Kwon H M, Bird J C and Varanasi K K 2013 *Appl. Phys. Lett.* **103** 201601
- [21] Tran T, Staat H J J, Susarrey-Arce A, Foertsch T C, Van Houselt A, Gardeniers H J G E, Prosperetti A, Lohse D and Sun C 2013 *Soft Matter.* **9** 3272
- [22] Del C D A, Marin A G, Romer G R, Pathiraj B, Lohse D and Huis A J 2012 *Langmuir* **28** 15106
- [23] Shahriari A, Wurz J and Bahadur V 2014 *Langmuir* **30** 12074
- [24] Clavijo C E, Crockett J and Maynes D 2017 *Int. J. Heat Mass Transfer* **108** 1714
- [25] Vakarelski I U, Patankar N A, Marston J O, Chan D Y and Thoroddsen S T 2012 *Nature* **489** 274
- [26] Méndez-Vilas A, Jódar-Reyes A B and González-Martín M L 2009 *Small* **5** 1366
- [27] Tabe H, Kobayashi K, Yaguchi H, Fujii H and Watanabe M 2020 *Int. J. Therm. Sci.* **150** 106203
- [28] Horne J E, Lavrik N V, Terrones H and Fuentes-Cabrera M 2015 *Sci. Rep.* **5** 11769
- [29] Tabe H, Kobayashi K, Yaguchi H, Fujii H and Watanabe M 2019 *Heat Mass Transfer* **55** 993
- [30] Rodrigues J and Desai S 2019 *Nanoscale* **11** 12139
- [31] Green M S 1954 *J. Chem. Phys.* **22** 398
- [32] Kubo R 1957 *J. Phys. Soc. Jpn.* **12** 570
- [33] Dong L, Wu X S, Hu Y, Xu X F and Bao H 2021 *Chin. Phys. Lett.* **38** 027202
- [34] Yu X X, Ma D K, Deng C C, Wan X, An M, Meng H, Li X B, Huang X M and Yang N 2021 *Chin. Phys. Lett.* **38** 014401
- [35] Zhu G P, Zhao C W, Wang X W and Wang J 2021 *Chin. Phys. Lett.* **38** 024401
- [36] Plimpton S 1995 *J. Comput. Phys.* **117** 1
- [37] Cui L, Feng Y, Tang J, Tan P and Zhang X 2016 *Int. J. Therm. Sci.* **99** 64
- [38] Jorgensen W L and Madura J D 1985 *Mol. Phys.* **56** 1381
- [39] Mahoney M W and Jorgensen W L 2000 *J. Chem. Phys.* **112** 8910
- [40] An M, Demir B, Wan X, Meng H, Yang N and Walsh T R 2019 *Adv. Theor. Simul.* **2** 1800153
- [41] Yenigun O and Barisik M 2019 *Int. J. Heat Mass Transfer* **134** 634
- [42] Swope W C, Andersen H C, Berens P H and Wilson K R 1982 *J. Chem. Phys.* **76** 637
- [43] Ryckaert J P and Bellemans A 1978 *Faraday Discuss. Chem. Soc.* **66** 95
- [44] Mao Y and Zhang Y 2014 *Appl. Therm. Eng.* **62** 607
- [45] Alexeev D, Chen J, Walther J H, Giapis K P, Angelikopoulos P and Koumoutsakos P 2015 *Nano Lett.* **15** 5744
- [46] Zong D, Yang Z and Duan Y 2017 *Appl. Therm. Eng.* **122** 71
- [47] Hua-Yi H, Lin M C, Bridget P, Lin C R, Patankar N A and Kumar M Y 2017 *PLoS One* **12** e0187175
- [48] Gong G M, Wu J T, Zhao Y, Liu J G, Jin X and Jiang L 2014 *Soft Matter* **10** 549